Journal of Computer Applications ISSN: 0974 – 1925,
Volume-5, Issue EICA2012-3, February 10, 2012

Retinal Blood Vessel Segmentation using Gray-Level and Moment Invariants-Based Features

Jegatha R
M.E Computer Science,
Rajiv Gandhi College of Engineering,
Chennai, India.
E-mail: jega.jeyavel@gmail.com

Lakshmi K
Assistant Professor ,
M.E Computer Science,
Rajiv Gandhi College of Engineering,
Chennai, India.

Abstract- Automatic blood vessel segmentation is an important issue for assessing retinal abnormality and diagnosis of many diseases. A new supervised method for blood vessel detection and segmentation in digital retinal images is based on Neural networks. Neural network (NN) scheme is meant for pixel classification and computes a 7-D vector composed of gray-level and moment invariants-based features for pixel representation. The method was evaluated on the publicly available DRIVE and STARE databases, widely used for this purpose, since they contain retinal images where the vascular structure has been precisely marked by experts. Blood vessel segmentation is performed through various stages: Preprocessing, Feature extraction, Classification and Post processing. The segmentation of vessels is difficult by huge variations in local contrast, particularly in case of the minor vessels. In this paper, we propose a new method of texture based vessel segmentation to overcome this problem. We use Gaussian and L*a*b* perceptually uniform color spaces with original RGB for texture feature extraction on retinal images. A bank of Gabor energy filters are used to analyze the texture features from which a feature vector is constructed for each pixel. The fuzzy C-means (FCM) clustering algorithm is used to classify the feature vectors into vessel or non-vessel based on the texture properties. From the FCM clustering output we attain the final output segmented image after a post processing step. We compare our method with hand-labeled ground truth segmentation of five images and achieve 84.37% sensitivity and 99.61% specificity.

Keywords: *Fuzzy C-means (FCM) clustering algorithm, gray-level, moment invariants-based features, Gaussian, Gabor energy filters Neural network (NN) scheme.*

I. INTRODUCTION

Retinal vessel occlusion is a blockage in the blood vessels of the eye that can cause sight loss. This information describes two different types of vessel occlusion and their affect on vision. A blockage in either a retinal vein or artery is medically known as a 'retinal vessel occlusion. Occlusion means closing or blocking up. They can happen in any of the blood vessels in the body, including the retinal arteries and veins. A retinal vessel occlusion can affect sight. This information describes the causes of retinal vessel occlusion, the effects they have on vision and any treatment that may be available. Because the occlusion can happen in either a vein or an artery they will be described separately.

Diabetes can affect sight by causing cataracts, glaucoma, and most importantly, damage to blood vessels inside the eye, a condition known as "diabetic retinopathy". Diabetic

retinopathy is a complication of diabetes that is caused by changes in the blood vessels of the retina. When blood vessels in the retina are damaged, they may leak blood and grow fragile, brush-like branches and scar tissue. This can blur or distort the vision images that the retina sends to the brain.

Diabetic eye disease is a leading cause of blindness in the United States. People with untreated diabetes are said to be 25 times more at risk for blindness than the general population. The longer a person has had diabetes, the higher the risk of developing diabetic retinopathy. Fortunately, with regular, proper eye care and treatment when necessary, the incidence of severe vision loss has been greatly reduced. If you have diabetes, your ophthalmologist can help to prevent serious vision problems.

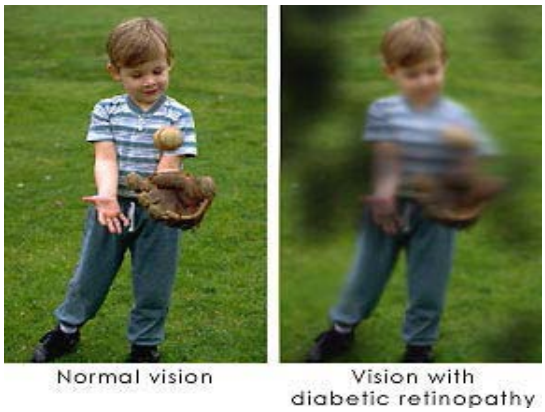

Figure 1: Image taken with Normal Eye and after the Diabetic Complexity

Most often, diabetic retinopathy has no symptoms until the damage to your eyes is severe. Symptoms of diabetic retinopathy include: Blurred vision and slow vision loss over time, Floaters, Shadows or missing areas of vision, Trouble seeing at night. Many people with early diabetic retinopathy have no symptoms before major bleeding occurs in the eye. Vessel assessment demands vascular tree segmentation from the background for further processing. Knowledge on blood vessel location can be used to reduce the number of false positives in micro aneurysm and hemorrhage detection. In this paper, a new methodology for blood vessel detection is presented. It is based on pixel classification using a 7-D feature vector extracted from preprocessed retinal images and given as input to a neural network.

Supervised methods for pixel classification feature vectors are formed by gray-scale values from a window centered on the pixel. Continuous wavelet transform (CWT) and integration of multi-scale information through supervised classification assists the accuracy of results . Here we improve on those methods using a Bayesian classifier with Gaussian mixture models as class likelihoods and evaluate performances with ROC analysis.

Each pixel is represented by a feature vector including measurements at different scales taken from the continuous two-dimensional Morlet wavelet transform. The resulting feature space is used to classify each pixel as either a vessel or non-vessel pixel. We use a Bayesian classifier with class-conditional probability density functions (likelihoods) described as Gaussian mixtures, yielding a fast classification. We enhance methods using vessel tracking, mathematical morphology, matched filtering, model-based locally adaptive thresholding or deformable models. A reference of the models' illustration can be understood from figure 2.Older methods includes mainly rule based methods. Rule-based methods, rule discovery or

rule extraction from data, are data mining techniques aimed at understanding data structures, providing comprehensible description instead of only black-box prediction. Rule based systems should expose in a comprehensible way knowledge hidden in data, providing logical justification for drawing conclusions, showing possible inconsistencies and avoiding unpredictable conclusions that black box predictors may generate in untypical situations. Sets of rules are useful if rules are not too numerous, comprehensible, and have less accuracy and includes redundancies. To overcome all the above mentioned deficiencies we propose supervised methods in our model. A supervised learning algorithm analyzes the training data and produces an inferred function, which is called a classifier (if the output is discrete, see classification) or a regression function (if the output is continuous, see regression). The inferred function should predict the correct output value for any valid input object. This requires the learning algorithm to generalize from the training data to unseen situations in a "reasonable" way.

II. MODEL FOR BLOOD VESSEL SEGMENTATION

The necessary feature vector is computed from preprocessed retinal images in the neighborhood of the pixel under consideration. The following process stages may be identified: 1) original fundus image preprocessing for gray-level homogenization and blood vessel enhancement, 2) feature extraction for pixel numerical representation, 3) application of a classifier to label the pixel as vessel or non vessel, and 4) post processing for filling pixel gaps in detected blood vessels and removing falsely-detected isolated vessel pixels.

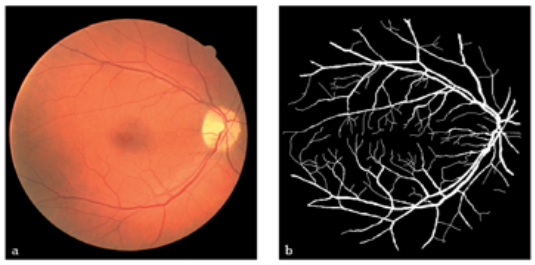

Figure 2: (a) Original retinal image , (b) Vessel Enhanced image.

Our methods are tested and evaluated on two publicly available databases of non-mydriatic images and corresponding manual segmentations: the DRIVE [1] and STARE [2] databases. The DRIVE database consists of images , along with manual segmentations of the vessels. The images are captured in digital form from a Canon CR5 non-mydriatic 3CCD camera at 45◦ field of view (FOV). The images are of size 768 × 584 pixels, 8 bits per color channel and have a FOV of approximately 540 pixels in diameter The images have been divided into a training and test set, each containing various images. The STARE database consists of 20 digitized slides captured by a TopCon TRV-50 fundus camera at 35◦ FOV. The slides were digitized to 700 × 605 pixels, 8 bits per color channel. The FOV in the images are approximately 650×550 pixels in diameter.

A. Preprocessing

In order to reduce the noise effects associated with the processing, the input image was preprocessed by a mean filter of size 5x5 pixels. Due to the circular shape of the non-mydriatic image boundary, neither the pixels outside the region-of-interest nor its boundary were considered, in order to avoid boundary effects. The pre-processing algorithm consists

of determining the pixels outside the aperture that are neighbors to pixels inside the aperture and replacing each of their values with the mean value of their neighbors inside the aperture. This process is repeated and can be seen as artificially increasing the area inside the aperture. Before the application of the wavelet transform to non-mydriatic images, we invert the green channel of the image, so that the vessels appear brighter than the background. Preprocessing proceeds with the following steps: 1) vessel central light reflex removal, 2) background homogenization, and 3) vessel enhancement.

1. Vessel Central Light Reflex Removal: Some blood vessels include a light streak (known as a light reflex) which runs down the central length of the blood vessel. Since retinal blood vessels appear darker than the background. According to the spatial gray properties of the optic disk and large blood vessels, automatic erasing the edges of the optic disk are implemented subsequently. The optic disk is the origin of blood vessels and the brightest region in retinal image. Large vessels are dark objects with two-sides boundary, relative to the background. In the gradient images convoluted with Sobel operators along horizontal and vertical directions, a large vessel always corresponds to a pair of local gradient maximum and minimum on both sides along a profile. And the edge of the optic disk corresponds to a single local maximum or minimum.

2. Background Homogenization: Background pixels may have different intensity for the same image and, although their gray-levels are usually higher than those of vessel pixels (in relation to green channel images), the intensity values of some background pixels is comparable to that of brighter vessel pixels. With the purpose of removing these background lightening variations, a shade-corrected image is accomplished from a background estimate. This image is the result of a filtering operation with a large arithmetic mean kernel. Firstly, a 3x 3 mean filter is applied to smooth occasional salt-and-pepper noise. Further noise smoothing is performed by convolving the resultant image with a Gaussian kernel of dimensions, mean and variance. Secondly, a background image , is produced by applying a 69x 69 mean filter. Finally, a shade-corrected image is obtained by transforming linearly values into integers covering the whole range of possible gray-levels (0 –255 , referred to 8-bit images).

3. Vessel Enhancement: The final preprocessing step consists on generating a new vessel-enhanced image , which proves more suitable for further extraction of moment invariants-based features . while bright retinal structures are removed (i.e., optic disc, possible presence of exudates or reflection artifacts), the darker structures remaining after the opening operation become enhanced (i.e., blood vessels, fovea, possible presence of micro aneurysms or hemorrhages).

B. Feature Extraction

Feature extraction is a special form of dimensionality reduction. When the input data to an algorithm is too large to be processed and it is suspected to be notoriously redundant (much data, but not much information) then the input data will be transformed into a reduced representation set of features. The aim of the feature extraction stage is pixel characterization by means of a feature vector, a pixel representation. In this paper, the following sets of features were selected.

- **Gray-level-based features:** Features based on the differences between the gray-level in the candidate pixel and a statistical value representative of its surroundings.

- **Moment invariants-based features***:* Features based on moment invariants for describing small image regions formed by the gray-scale values of a window centered on the represented pixels. A wavelet transform can be defined as Eq.1, where $\Psi a,\ b$ is the wavelet with scale a, location b by dilations and translations from mother wavelet Ψ centered on the origin. Similarly, a curve let transform can be defined as Eq.2. Here $\Psi a,\ b,\ \theta$ is a curve let with scale a, location b and direction θ, which can be regarded as a wavelet $\Psi a,$ stretched preferentially in direction θ [9].

$$Wf(a,b) = \langle \psi_{a,b}, f \rangle$$

C. Classification

In the feature extraction stage, each pixel from a fundus image is characterized by a vector in a 7-D feature space Supervised classification has been applied to obtain the final segmentation, with the pixel classes defined as C1 = {vessel pixels} and C2 = {non-vessel pixels}. In order to obtain the training set, several fundus image have been manually segmented, allowing the creation of a labeled training set into classes C1 and C2 (see Subsection II-A). Due to the computational cost of training the classifiers and the large number of samples, we randomly select a subset of the available samples to use for actually training the classifiers. We will present results for two different classifiers, described below.

Gaussian mixture model Bayesian classifier: We have achieved very good results using a Bayesian classifier in which each class-conditional probability density function (likelihood)is described as a linear combination of Gaussian functions [41], [42]. We will call this the Gaussian mixture model (GMM) classifier. The Bayes classification rule for a feature vector v can be stated in terms of posterior probabilities as

Decide C1 if P(C1|v) > P(C2|v);
Otherwise, decide C2
We recall Bayes rule:
P(Ci|v) =p(v|Ci)P(Ci)p(v)
where p(v|Ci) is the class-conditional probability density function, also known as likelihood, P(Ci) is the prior probability of class Ci, and p(v) is the probability density function of v (sometimes called evidence).To obtain a decision rule based on estimates from our training set, we apply Bayes rule to Eq. 2, obtaining the equivalent decision rule:

Decide C1 if p(v|C1)P(C1) > p(v|C2)p(C2);
otherwise, decide C2
We estimate P(Ci) as Ni/N, the ratio of class i samples in the training set. The class likelihoods are described as linear combinations of Gaussian functions:
p(v|Ci) =kiXj=1p(v|j,Ci)Pj
where ki is the number of Gaussians modeling likelihood i,
Pj is the weight of Gaussian j and each p(v|j,Ci) is a dimensional Gaussian distribution. All the described rules are illustrated through Images on processing in figure 3 as follows,

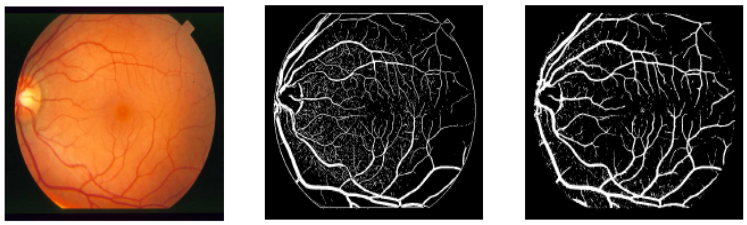

Figure 3: Images after the clustering and Classification.

Two classification stages can be distinguished: a design stage, in which the NN configuration is decided and the NN is trained, and an application stage, in which the trained NN is used to classify each pixel as vessel or non vessel to obtain a vessel binary image.

1. Neural Network Design: A multilayer feed forward network, consisting of an input layer, three hidden layers and an output layer, is adopted in this paper. The input layer is composed by a number of neurons equal to the dimension of the feature vector (seven neurons). Regarding the hidden layers, several topologies with different numbers of neurons were tested. A number of three hidden layers, each containing 15 neurons, provided optimal NN configuration. The output layer contains a single neuron and is attached.

2. Neural Network Application*:* At this stage, the trained NN is applied to an "unseen" fundus image to generate a binary image in which blood vessels are identified from retinal background: pixels' mathematical descriptions are individually passed through the NN.

D. Postprocessing

Classifier performance is enhanced by the inclusion of a two step postprocessing stage: the first step is aimed at filling pixel gaps in detected blood vessels, while the second step is aimed at removing falsely detected isolated vessel pixels. The output produced by the classifier leads to a binary image where each pixel is labeled as vessel or non-vessel. Some misclassified pixels appeared as undesirable noise in the classified image. In addition, for some vessels, only their boundaries were classified, so that it was necessary to perform post-processing by using morphological tools to obtain the final desired segmentation. Finally, to optimize the vessel contours, morphological operations have been applied, beginning by area open to eliminate small noisy components.

III. SUMMARY

In this paper, we present a novel automatic blood vessel detection algorithm for retinal images acquired from diabetic retinopathy screening programs. A Brief summary is given in the figure 4.The results we have obtained suggest that pixel-level classification in conjunction with Gabor filter responses, feature extraction and SVMs classifiers can provide robust and computationally efficient blood vessel segmentation while suppressing the backgrounds.

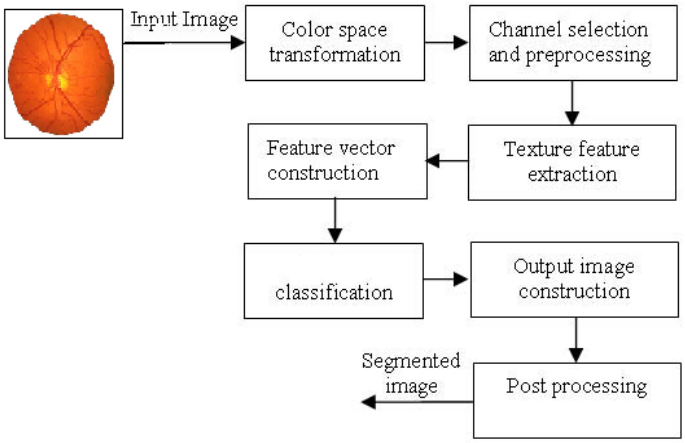

Figure 4: Flow Diagram for the Proposed Segmentation Algorithm.

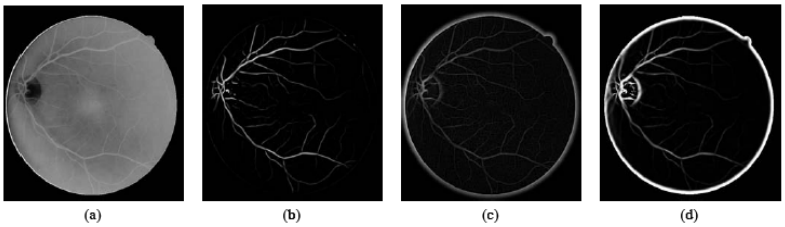

Figure 5: (a) Input image(Original Green Channel), (b) Vessel Enhanced Image, (c) Noise Filter Image ,(d) Edge Enhanced Image.

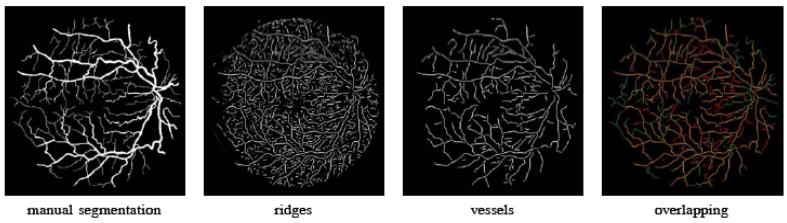

Figure 6 :Various Stages of Segmentation from Manual to Ridges and to Overlapping Vessels Including Neural Network Classified Image (Post Processed Image).

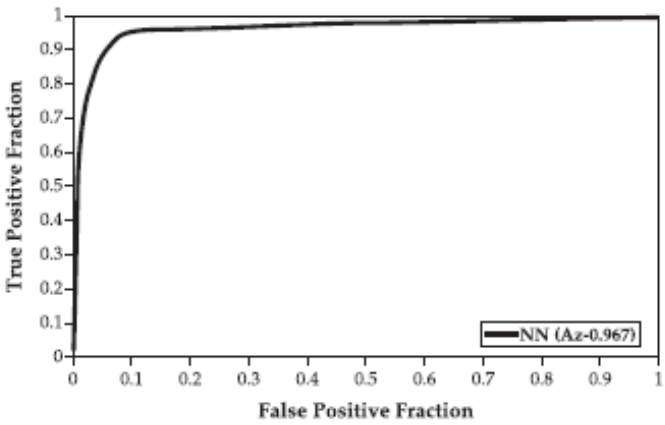

Figure 7: Optimum Neual Network Based Receiver Operating Characteristic Curve

IV. EXPERIMENTS AND RESULTS

A. Dataset and Experiment Settings

Here, a balanced dataset of vascular and non-vascular pixels was established to eliminate any possible bias towards either of the two classes. Our representative learning dataset comprised of 125,000 vessel and 125,400 non-vessel pixels randomly collected from 20 retinal images. This dataset was then divided into a training set, a validation set, and a test set in a 65:10:25 ratio. We employed a three-layer perceptron NN with a 15 node input layer corresponding to our feature vector. We experimented with a hidden layer with a range of 2 to 20 hidden units to find the optimum architecture. A single output node gave the final classification probability. The network was trained using standard Back-Propagation learning method.12 The classifier error was calculated using pixels from validation set after each iteration of training.

The NN performance was measured using the previously unseen features from the test set in the usual terms of sensitivity and specificity. Sensitivity is the ratio of true positive (TP) decisions to all positive decisions, while specificity is the ratio of true negative (TN) decisions to all negative decisions. Another reported measure, the accuracy, is the ratio between the total numbers of correctly classified vascular pixels to all instances existing in the test set. The classical tool to achieve tradeoff between sensitivity and specificity criteria is the Receiver Operating Characteristics (ROC) curve, which is shown in the fig 7. This curve is typically plotted with the TP fraction against the FP fraction. The bigger the area under the ROC curve (Az), the higher the probability of making a correct decision. Figure 7 compares the behavior of the optimum NN classifier for the full range of output threshold values. The optimum NN classifier achieved very good performance with Az value of 0.967.

B. Results

Overall, the classification analysis indicated that the best optimum classifier for distinguishing vascular pixels is a NN classifier with 10 hidden units. The second best performance was achieved by various classifiers. Typical abnormal retinal image from the image dataset that has been classified at pixel level using the optimum NN classifier and various processes. The majority of large and small vessels were detected; there was erroneous detection of noise and other artifacts. The overall segmentation process is illustrated through figure 5 and 6.The majority of errors were due to background noise and non-uniform illumination across the retinal images, the border of the optic disc. Those noises could easily be overcome through four processing stages.

V. CONCLUSION

Our proposed vessel extraction technique does not require any user intervention, and has consistent performance in both normal and abnormal images. Higher accuracy than that of other previously can be reported vessel segmentation methods. The results demonstrated herein indicate that automated identification of retinal blood vessels based on Gabor filter responses and NN classifiers can be very successful. Hence, eye care specialists can potentially monitor larger populations using this method. Furthermore, observations based on such a tool would be systematically reproducible.

VI. ACKNOWLEDGEMENT

We wish to express our sincere thanks to all the staff member of C.S.E Department, Rajiv Gandhi College of Engineering for their help and cooperation.

REFERENCES

1. H. R. Taylor and J. E. Keeffe, "World blindness: A 21st century perspective," *Br. J. Ophthalmol.*, vol. 85, pp. 261–266, 2001.
2. R. Klein, S. M. Meuer, S. E. Moss, and B. E. Klein, "Retinal micro aneurysm counts and 10-year progression of diabetic retinopathy," *Arch. Ophthalmol.*, vol. 113, pp. 1386–1391, 1995.
3. P. Massin, A. Erginay, and A. Gaudric*, Retinopathies Diabétique*. New York: Elsevier, 2000.
4. S. Wild, G. Roglic, A. Green, R. Sicree, and H. King, "Global prevalence of diabetes: Estimates for the year 2000 and projections for 2030," *Diabetes Care*, vol. 27, pp. 1047–1053, 2004.
5. S. J. Lee, C. A. McCarty, H. R. Taylor, and J. E. Keeffe, "Costs of mobile screening for diabetic retinopathy: A practical framework for rural populations," *Aust. J. Rural Health*, vol. 8, pp. 186–192, 2001.
6. D. S. Fong, L. Aiello, T. W. Gardner, G. L. King, G. Blankenship, J. D. Cavallerano, F. L. Ferris, and R. Klein, "Diabetic retinopathy," *Diabetes Care*, vol. 26, pp. 226–229, 2003.
7. "Economic costs of diabetes in the U.S. in 2007," in *Diabetes Care*. : American Diabetes Association, 2008, vol. 31, pp. 596–615.
8. American Academy of Ophthalmology Retina Panel, Preferred Practice Pattern Guidelines. Diabetic Retinopathy. San Francisco, CA, Am. Acad. Ophthalmo., 2008 [Online]. Available:http://www.aao.org/ppp
9. J. J. Kanski, Clinical Ophthalmology: A systematic approach. London: Butterworth-Heinemann, 1989.
10. E. J. Sussman, W. G. Tsiaras, and K. A. Soper, "Diagnosis of diabetic eye disease," Journal of the American Medical Association, vol. 247,pp. 3231–3234, 1982.
11. S. J. Lee, C. A. McCarty, H. R. Taylor, and J. E. Keeffe, "Costs of mobile screening for diabetic retinopathy: A practical framework for rural populations," Aust J Rural Health, vol. 8, pp. 186–192, 2001.
12. H. R. Taylor and J. E. Keeffe, "World blindness: a 21st century perspective," British Journal of Ophthalmology, vol. 85, pp. 261–266, 2001.
13. C. P. McQuellin, H. F. Jelinek, and G. Joss, "Characterization of fluorescein angiograms of retinal fundus using mathematical morphology: a pilot study," in 5th International Conference on Ophthalmic Photography, Adelaide, 2002, p. 152.
14. L. Streeter and M. J. Cree, "Micro aneurysm detection in color fundus images," in Image and Vision Computing New Zealand, Palmerstone North, New Zealand, November 2003, pp. 280–284.
15. T. Y. Wong, W. Rosamond, P. P. Chang, D. J. Couper, A. R. Sharrett, L. D. Hubbard, A. R. Folsom, and R. Klein, "Retinopathy and risk of congestive heart failure," Journal of the American Medical Association, vol. 293, no. 1, pp. 63–69, 2005.

16. http://www.raycosecurity.com/biometrics/EyeDentify.html.
17. W.-S. Chen, K.-H. Chih, S.-W. Shih, and C.-M. Hsieh, “Personal identification technique based on human Iris recognition with wavelet transform,” in Proceedings of IEEE International Conference on Acoustics, Speech and Signal Processing (ICASSP ’05), vol. 2, pp. 949–952, Philadelphia, Pa, USA, March 2005.

BIOGRAPHY

R.Jegatha received B.E in computer science at SRR Engineering College, Chennai. Now Pursuing M.E at Rajiv Gandhi College of Engineering. Her research interests include medical image processing, pattern recognition, and Neural networks .